

Focusing of aberrated, partially coherent, square, flat-topped pulsed beams by a thin lens

Guowen Zhang (张国文)¹, Xingqiang Lu (卢兴强)^{1*}, Shenlei Zhou (周申蕾)¹,
Weixin Ma (马伟新)², and Jian Zhu (朱俭)²

¹National Laboratory on High Power Laser and Physics, Shanghai Institute of Optics and Fine Mechanics, Chinese Academy of Sciences, Shanghai 201800, China

²Shanghai Institute of Laser Plasmas, Shanghai 201800, China

*Corresponding author: xingqianglu@siom.ac.cn

Received September 28, 2013; accepted October 14, 2013; posted online February 27, 2014

Flat-topped beam theoretical model and unified theory of coherence and polarization of light are used as the bases in examining aberrated, partially coherent, electromagnetic, square, flat-topped pulsed beams focused by a thin lens. This study demonstrates that Astigmatism is not necessarily undesirable in certain circumstances, and a certain amount of astigmatism can be guaranteed a similar spatial envelope of the beams in the geometric focal plane as the source of aberrated, partially coherent, electromagnetic, square, flat-topped pulsed beams. This feature may be useful in determining the fidelity of high-power laser-beam transmission areas.

OCIS codes: 140.3295, 140.3430, 260.1960, 260.2110.

doi: 10.3788/COL201412.S11401.

Laser beams with square, flat-topped spatial profile are required to improve the energy efficiency of inertial confined fusion high-power laser systems and to make use of optical energy adequately. Several theoretical models have been proposed to describe laser beams with a flat-topped spatial profile. The super-Gaussian beam is the first laser beam proposed^[1]. In 1994, Gori^[2] and Bagini *et al.*^[3] proposed another model called the flattened Gaussian beam, the field of which can be expressed as a finite sum of Laguerre–Gaussian model or Hermite–Gaussian model. Recently, Li proposed a new theoretical model to describe a flat-topped light beam by expressing its electric field as a finite sum of fundamental Gaussian beams^[4,5]. Cai *et al* proposed an elliptical flat-topped beam to describe an elliptically symmetric flat-topped beam by expressing its electric field as a finite sum of astigmatic, elliptical Gaussian beams^[6]. However, at present, most studies on flat-topped beams have been confined to circular, flat-topped beams, while research on square, flat-topped, spatial-profile beams has been scarce^[7–17]. Partially coherent, square, flat-topped pulsed beams are shown to be practical models for high-power laser drivers since most light beams can be described with the use of partially coherent beams^[18]. As is known, aberrations may emerge as a laser beam passes through an optical system or atmosphere, or they could be inherent, as in the case of laser diode astigmatism. In this case, the propagation characteristics of the beams with aberrations need to be examined further, such as stochastic electromagnetic beams, Laguerre–Gaussian beams, and partially coherent, flat-topped beams, among others. These beams with aberrations have been studied^[19–22]. In other aspects, laser beams propagating through an aberrated optical system have also been presented^[23–29]. However,

to our knowledge, no research has been made on the influence of aberration on partially coherent, electromagnetic, square, flat-topped pulsed beams in a focused field before. In this study, we investigate the changes in aberrated, partially coherent, electromagnetic, square, flat-topped pulsed beams in the focused field, with astigmatic aberration duly taken into account. First, this astigmatic aberration is taken as a phase function that modifies the wave-front of the light beam. Second, we derive an analytical expression for this beam that propagates through a thin lens, based on which spectral density is investigated and expounded in detail.

In space–time domain, the electric mutual coherence matrix of a stochastic spatially and spectrally partially coherent electromagnetic pulsed beam at the source plane $z = 0$ is given by

$$\begin{aligned} \bar{\Gamma}^{(0)}(\boldsymbol{\rho}_1, \boldsymbol{\rho}_2, t_1, t_2) \\ = \begin{bmatrix} \Gamma_{xx}^{(0)}(\boldsymbol{\rho}_1, \boldsymbol{\rho}_2, t_1, t_2) & \Gamma_{xy}^{(0)}(\boldsymbol{\rho}_1, \boldsymbol{\rho}_2, t_1, t_2) \\ \Gamma_{yx}^{(0)}(\boldsymbol{\rho}_1, \boldsymbol{\rho}_2, t_1, t_2) & \Gamma_{yy}^{(0)}(\boldsymbol{\rho}_1, \boldsymbol{\rho}_2, t_1, t_2) \end{bmatrix}, \end{aligned} \quad (1)$$

where

$$\begin{aligned} \Gamma_{ij}^{(0)}(\boldsymbol{\rho}_1, \boldsymbol{\rho}_2, t_1, t_2) &= \langle E_i^*(\boldsymbol{\rho}_1, t_1) E_j(\boldsymbol{\rho}_2, t_2) \rangle \\ &= \sqrt{I_i^{(0)}(\boldsymbol{\rho}_1, t_1)} \sqrt{I_j^{(0)}(\boldsymbol{\rho}_2, t_2)} \eta_{ij}^{(0)}(\boldsymbol{\rho}_1 - \boldsymbol{\rho}_2, t_1 - t_2), \\ &(i = x, y; j = x, y) \end{aligned} \quad (2)$$

where $E_i^{(0)}$ and $E_j^{(0)}$ are the components of the electric field $E(\boldsymbol{\rho}, t)$ at $z = 0$ plane, $\boldsymbol{\rho}$ is the transverse position vector (perpendicular to the z -axis), and t is the time. The asterisk denotes the complex conjugation, and the angular brackets denote the ensemble average. $\Gamma_{ij}^{(0)}(\boldsymbol{\rho}, t)$ represents the elements of the cross-spectral

density matrix, which generates a beam in half-space $z > 0$. $I_i^{(0)}$ is the spatial spectral density of the component $E_i^{(0)}$ in the electric field. In most cases, $I_i^{(0)}$ is expressed as a Gaussian-type distribution. Considering the light beam with flat-topped profile, the intensity distribution can be expressed as^[4,5]

$$I_i^{(0)}(\mathbf{p}, t) = A_i \exp\left\{-\frac{t^2}{T_0^2}\right\} \sum_{m=1}^N \alpha_m \exp\left\{-m\beta_m \frac{\mathbf{p}^2}{2\sigma^2}\right\}, \quad (3)$$

where

$$\alpha_m = (-1)^{m+1} \frac{N!}{m!(N-m)!}, \quad (3a)$$

$$\beta_m = \sum_{m=1}^N \frac{\alpha_m}{m}, \quad (3b)$$

and $\eta_{ij}^{(0)}$ is the spectral degree of correlation between the components $E_i^{(0)}$ and $E_j^{(0)}$ given by the expressions

$$\eta_{ij}^{(0)}(\mathbf{p}_1 - \mathbf{p}_2, t_1 - t_2) = B_{ij} \exp\left\{-\frac{(\mathbf{p}_1 - \mathbf{p}_2)^2}{2\delta_{ij}^2}\right\} \times \exp\left\{-\frac{(t_1 - t_2)^2}{2T_{ci}^2}\right\} \exp\{i\omega_0(t_1 - t_2)\}, \quad (4)$$

where

$$\begin{cases} B_{ij} \equiv 1 & \text{when } i = j, \\ |B_{ij}| \leq 1 & \text{when } i \neq j. \end{cases} \quad (4a)$$

In these expressions, the parameters A_i , B_{ij} , σ , and δ_{ij} generally depend on the carrier frequency ω_0 . The quantities σ and δ_{ij} represent the effective widths of spectral density $I_i^{(0)}$ and correlation $\eta_{ij}^{(0)}$, respectively. N is an integer, which is the order parameter of the partially coherent, flat-topped pulsed beams. T_0 is the pulse duration, and T_{ci} describes the temporal coherence length of the i component of the electric vector.

The electric vector components in the x and y directions are assumed as uncorrelated at plane $z = 0$ in order to simplify the analysis, i.e.,

$$\Gamma_{xy}^{(0)}(\mathbf{p}_1, \mathbf{p}_2, t_1, t_2) = \Gamma_{yx}^{(0)}(\mathbf{p}_1, \mathbf{p}_2, t_1, t_2) = 0. \quad (5)$$

With Fourier transform,

$$W_{ii}^{(0)}(\mathbf{p}_1, \mathbf{p}_2, \omega_1, \omega_2) = \frac{1}{(2\pi)^2} \int_{-\infty}^{\infty} \int_{-\infty}^{\infty} \Gamma_{ii}^{(0)}(\mathbf{p}_1, \mathbf{p}_2, t_1, t_2) \exp\{-i(\omega_1 t_1 - \omega_2 t_2)\} dt_1 dt_2, \quad (6)$$

the cross-spectral density matrix at plane $z = 0$ can be derived and given by

$$\overline{W}^{(0)}(\mathbf{p}_1, \mathbf{p}_2, \omega_1, \omega_2) = \left[\left\langle W_{ii}^{(0)}(\mathbf{p}_1, \mathbf{p}_2, \omega_1, \omega_2) \right\rangle \right], \quad (7)$$

where

$$\begin{aligned} W_{ii}^{(0)}(\mathbf{p}_1, \mathbf{p}_2, \omega_1, \omega_2) &= \frac{T_0 A_i}{2\pi\Omega_{0i}} \sum_{m_1=1}^N \sum_{m_2=1}^N \alpha_{m_1} \alpha_{m_2} \exp\left\{-m_1\beta_1 \frac{\mathbf{p}_1^2}{4\sigma^2}\right\} \\ &\exp\left\{-m_2\beta_2 \frac{\mathbf{p}_2^2}{4\sigma^2}\right\} \times \exp\left\{-\frac{(\mathbf{p}_1 - \mathbf{p}_2)^2}{2\delta_{ii}^2}\right\} \\ &\exp\left\{-\frac{(\omega_1 - \omega_0)^2 + (\omega_2 - \omega_0)^2}{2\Omega_{0i}^2}\right\} \exp\left\{-\frac{(\omega_1 - \omega_2)^2}{2\Omega_{ci}^2}\right\}, \end{aligned} \quad (7a)$$

$$\Omega_{0i} = \sqrt{\frac{1}{T_0^2} + \frac{2}{T_{ci}^2}}, \quad (7b)$$

$$\Omega_{ci} = \frac{T_{ci}}{T_0} \Omega_{0i}, \quad (7c)$$

where Ω_{0i} and Ω_{ci} represent the spectral width and the spectral coherence width of the i component of the electric vector, respectively. Eqs. (7b) and (7c) give the relation of the pulse duration T_0 , temporal coherence length T_{ci} , spectral width Ω_{0i} , and spectral coherence width Ω_{ci} . The spectral coherence width Ω_{ci} is a measure of the correlation between different frequency components of the i component of the electric vector.

However, in Eq. (7a), the flat-topped beam is a circular flat-topped beam rather than a square type, which needs modification. In this study, an astigmatic aberrant source is taken into consideration. Various beams with different spectral distributions are modulated with a combination of optical systems, so the aberrations of the sources may be produced to a certain extent. Hence, it is critical to investigate the effect of the observation on the propagation properties of the source beams. The wave aberration function for astigmatism is characterized by

$$\Phi(x, y) = C_6 (y^2 - x^2), \quad (8)$$

where C_6 is the astigmatism coefficient. For simplicity, other aberrations are not considered in this study.

Therefore, Eq. (7) is transformed as

$$\begin{aligned} W_{ii}^{(0)}(x_1, y_1, x_2, y_2, \omega_1, \omega_2) &= \frac{T_0 A_i}{2\pi\Omega_{0i}} \\ &\exp\left\{-\frac{(\omega_1 - \omega_0)^2 + (\omega_2 - \omega_0)^2}{2\Omega_{0i}^2}\right\} \exp\left\{-\frac{(\omega_1 - \omega_2)^2}{2\Omega_{ci}^2}\right\} \\ &\times \exp\left\{-\frac{(x_1 - x_2)^2 + (y_1 - y_2)^2}{2\delta_{ii}^2}\right\} \\ &\exp\left\{\frac{i}{C} [\omega_1 \Phi(x_1, y_1) - \omega_2 \Phi(x_2, y_2)]\right\} \end{aligned}$$

$$\sum_{m_1=1}^N \sum_{m_2=1}^N \sum_{n_1=1}^N \sum_{n_2=1}^N \alpha_{m_1} \alpha_{m_2} \alpha_{n_1} \alpha_{n_2} \exp \left\{ - \left(m_1 \beta_{m_1} \frac{x_1'^2}{4\sigma^2} + m_2 \beta_{m_1} \frac{x_2'^2}{4\sigma^2} + n_1 \beta_{n_1} \frac{y_1'^2}{4\sigma^2} + n_2 \beta_{n_2} \frac{y_2'^2}{4\sigma^2} \right) \right\}, \quad (9)$$

where one of the key steps is the separation of coordinates x and y . The substance of the square flat-topped beam is the superposition of two sections of waves.

The propagation of the cross-spectral density matrix through a paraxial optical ABCD system follows a well-known propagation:

$$\begin{aligned} W_{ii}(x_1, y_1, x_2, y_2, z; \omega_1, \omega_2) &= \frac{\omega_1 \omega_2}{4\pi^2 c^2 B^2} \exp \left\{ \frac{i(\omega_2 - \omega_1)z}{c} \right\} \\ &\times \int_{-\infty}^{\infty} \int_{-\infty}^{\infty} \int_{-\infty}^{\infty} W_{ii}^{(0)}(x_1', y_1', x_2', y_2', \omega_1, \omega_2) \\ &\exp \left\{ - \frac{iC_6}{c} \left[(\omega_1 x_1'^2 - \omega_2 x_2'^2) - (\omega_1 y_1'^2 - \omega_2 y_2'^2) \right] \right\} \\ &\exp \left\{ \frac{i\omega_2}{2cB} \left[A(x_2'^2 + y_2'^2) - 2(x_2 x_2' + y_2 y_2') + D(x_2^2 + y_2^2) \right] \right. \\ &\left. - \frac{i\omega_1}{2cB} \left[A(x_1'^2 + y_1'^2) - 2(x_1 x_1' + y_1 y_1') + D(x_1^2 + y_1^2) \right] \right\} \\ &dx_1' dy_1' dx_2' dy_2', \quad (10) \end{aligned}$$

where c is the speed of light in vacuum, and A, B and D are elements of the transfer matrix $\begin{bmatrix} \mathbf{A} & \mathbf{B} \\ \mathbf{C} & \mathbf{D} \end{bmatrix}$. When

the aberrated, partially coherent, square, flat-topped pulsed beam passes through a thin lens at $z = 0$ plane, the transfer matrix is expressed as

$$\begin{bmatrix} \mathbf{A} & \mathbf{B} \\ \mathbf{C} & \mathbf{D} \end{bmatrix} = \begin{bmatrix} \mathbf{1} - \frac{z}{f} & \mathbf{z} \\ -\frac{1}{f} & \mathbf{1} \end{bmatrix}, \quad (11)$$

where f is the focal length of the thin lens located at $z = 0$ plane. Substituting Eqs. (8) and (11) into Eq. (10) after a series of integral calculations then gives

$$\begin{aligned} W_{ii}(x_1, y_1, x_2, y_2, z; \omega_1, \omega_2) &= A_i \frac{T_0 \omega_1 \omega_2}{8\pi c^2 z^2 \Omega_{0i}} \\ &\times \exp \left\{ - \frac{(\omega_1 - \omega_0)^2 + (\omega_2 - \omega_0)^2}{2\Omega_{0i}^2} \right\} \exp \left\{ - \frac{(\omega_1 - \omega_2)^2}{2\Omega_{ci}^2} \right\} \\ &\times \exp \left\{ \frac{i(\omega_2 - \omega_1)z}{c} \right\} \exp \left\{ \frac{i}{2zc} [\omega_2(x_2^2 + y_2^2) - \omega_1(x_1^2 + y_1^2)] \right\} \end{aligned}$$

$$\begin{aligned} &\times \sum_{m_1=1}^N \sum_{m_2=1}^N \sum_{n_1=1}^N \sum_{n_2=1}^N \frac{\alpha_{m_1} \alpha_{m_2} \alpha_{n_1} \alpha_{n_2}}{\sqrt{p_{m_1} p_{m_2} p_{n_1} p_{n_2}}} \\ &\exp \left\{ - \left[\left(1 + \frac{1}{4\delta_{ii}^4 p_{m_1} p_{m_2}} \right) \frac{\omega_1^2 x_1^2}{4z^2 c^2 p_{m_1}} \right. \right. \\ &\left. \left. - \frac{\omega_1 \omega_2 x_1 x_2}{4z^2 c^2 \delta_{ii}^2 p_{m_1} p_{m_2}} + \frac{\omega_2^2 x_2^2}{4z^2 c^2 p_{m_2}} \right] \right. \\ &\left. \exp \left\{ - \left[\left(1 + \frac{1}{4\delta_{ii}^4 p_{n_1} p_{n_2}} \right) \frac{\omega_1^2 y_1^2}{4z^2 c^2 p_{n_1}} \right. \right. \right. \\ &\left. \left. - \frac{\omega_1 \omega_2 y_1 y_2}{4z^2 c^2 \delta_{ii}^2 p_{n_1} p_{n_2}} + \frac{\omega_2^2 y_2^2}{4z^2 c^2 p_{n_2}} \right] \right\}, \quad (12) \end{aligned}$$

where,

$$p_{m_1} = \frac{m_1 \beta_{m_1}}{4\sigma^2} + \frac{1}{2\delta_{ii}^2} + \frac{(f-z)\omega_1 i}{2zcf} + \frac{C_6 \omega_1 i}{c}, \quad (12a)$$

$$p_{m_2} = \frac{m_2 \beta_{m_2}}{4\sigma^2} + \frac{1}{2\delta_{ii}^2} - \frac{(f-z)\omega_2 i}{2zcf} - \frac{C_6 \omega_2 i}{c} - \frac{1}{4\delta_{ii}^4 p_{m_1}}, \quad (12b)$$

$$p_{n_1} = \frac{n_1 \beta_{n_1}}{4\sigma^2} + \frac{1}{2\delta_{ii}^2} + \frac{(f-z)\omega_1 i}{2zcf} - \frac{C_6 \omega_1 i}{c}, \quad (12c)$$

$$p_{n_2} = \frac{n_2 \beta_{n_2}}{4\sigma^2} + \frac{1}{2\delta_{ii}^2} - \frac{(f-z)\omega_2 i}{2zcf} + \frac{C_6 \omega_2 i}{c} - \frac{1}{4\delta_{ii}^4 p_{n_1}}, \quad (12d)$$

On the basis of the unified theory of coherence and polarization introduced by Wolf, the spectral density of partially coherent, square, flat-topped pulsed beams is expressed as

$$\begin{aligned} S(x, y, \omega) &= Tr \left[\overline{W}(x, y, x, y, \omega, \omega) \right] \\ &= W_{xx}(x, y, x, y, \omega, \omega) + W_{yy}(x, y, x, y, \omega, \omega), \quad (13) \end{aligned}$$

where Tr is the trace of the cross-spectral density matrix. Eq. (12) represents the main analytical result obtained in this study. Eqs. (12) and (13) describe the changes in spectral density of the partially coherent, square, flat-topped pulsed beams from $z = 0$ plane to z -plane in the focused field, which depends on the astigmatism coefficient C_6 , spatial correlation parameter δ_{ii} , frequency ω , pulse duration T_0 , temporal coherence length T_{c_i} , and propagation distance z .

We now illustrate the propagation properties of the aberrated, partially coherent, electromagnetic, square, flat-topped pulsed beams through an unapertured thin lens with the use of some numerical examples. For simplification in our calculations, $A_x = A_y = 1$, $\sigma = 5$ mm, $\delta_{xx} = \delta_{yy} = \delta$, $T_{cx} = T_{cy} = T_c$, $\omega_0 = 3.106$ rad/fs, and $f = 500$ mm are fixed. First, we present the spatial spectral density distribution in the source plane. Fig. 1(a) and 1(b) show the spatial spectral density

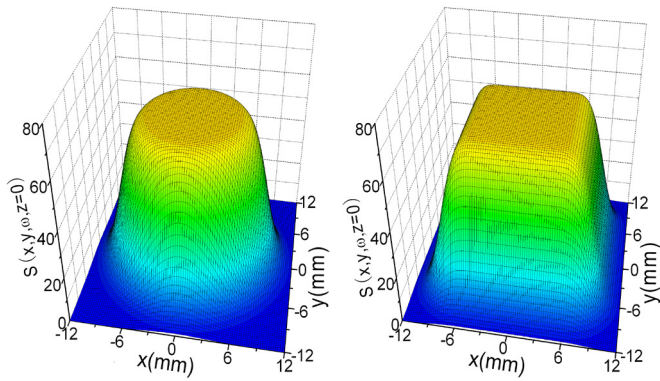


Fig. 1. (Color online) Spatial spectral density distribution in the source plane. Calculated (a) using Eq. (7) and (b) Eq. (8). $\delta = 1$ mm, $T_0 = 70$ fs, $T_c = 4$ fs, $\omega = \omega_0$, and $N = 10$.

of the flat-topped light beams with Eqs. (7) and (8), respectively. As indicated in Fig. 1, Eq. (8), which is derived from Eq. (7), shows a good spatial distribution of the square flat-topped light beam.

This study aims to examine how the parameters of the light source affect the spatial spectral density distribution of the aberrated, partially coherent, square, flat-topped pulsed beams in the focused field. Fig. 2 shows the distribution of the spectral density of the aberrated, partially coherent, square, flat-topped pulsed beams in the $z-x$ plane. Fig. 2 shows that astigmatism affects the spatial spectral density, and the distribution of the spatial spectral density is different for different values of C_6 . In Fig. 3, we present the spectral density of the aberrated, partially coherent, square, flat-topped pulsed beams in the $z-y$ plane. The corresponding results in the aberration-free case of $C_6 = 0$ and the distribution of the spectral density in the $z-y$ plane are depicted in Fig. 3(a), which are similar to the behavior in the

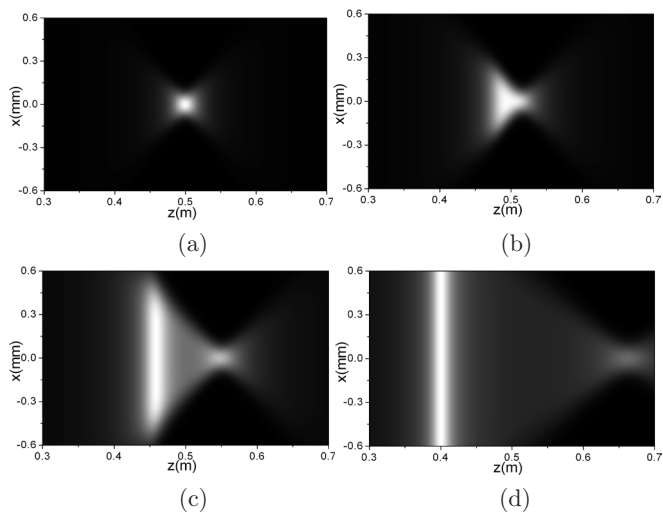


Fig. 2. Spectral density distribution in $z-x$ plane. (a) $C_6 = 0$ m^{-1} , (b) $C_6 = 0.01$ m^{-1} , (c) $C_6 = 0.03$ m^{-1} , and (d) $C_6 = 0.08$ m^{-1} . The other parameters are the same as in Fig. 1.

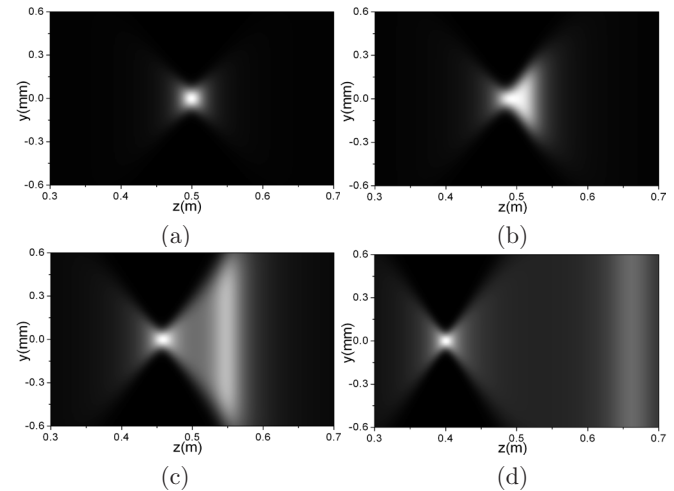


Fig. 3. Spectral density distribution in $z-y$ plane. (a) $C_6 = 0$ m^{-1} , (b) $C_6 = 0.01$ m^{-1} , (c) $C_6 = 0.03$ m^{-1} , and (d) $C_6 = 0.08$ m^{-1} . The other parameters are the same as in Fig. 1.

$z-x$ plane in Fig. 2(a). In the case of $C_6 \neq 0$, the distribution of the spectral density in the $z-y$ plane is different from that in the $z-x$ plane, and that in the $z-y$ plane is likely to turn over the distribution of the spectral density right and left around 0.5 m. However, it is clearly characterized by a strong spectral density distribution between the geometric focal plane and the light source plane. This effect is called focal shift, which can be mainly attributed to astigmatism of the pulsed beams.

Fig. 4 presents the three-dimensional (3D) irradiance spectral density distribution in the $x-y$ plane in the aberration case of $C_6 = 0.03$ m^{-1} . With astigmatism, the spectral density profile are not square but rectangle, except in the geometric focal plane. We can also observe two strong areas around $z = 0.45$ m and $z = 0.55$ m based on the value of the spectral density.

The contours of the spectral density for different values of δ are presented in Fig. 5. Astigmatism is more obvious with an increase in δ . Fig. 6 shows the 3D irradiance distribution of the spectral density for different values of C_6 . Fig. 6 shows two stronger areas that are widely separated as the astigmatism coefficient increases.

The influence of the astigmatism coefficient C_6 on the frequency is presented in Fig. 7. Notably, one strong area is split into two strong areas in the focused field, and two strong areas are widely separated with an increase in astigmatism coefficient. Fig. 8 shows the influence of the coherence length δ on the frequency for the astigmatism coefficient $C_6 = 0.03$ mm^{-1} . One strong area is also found to split into two stronger areas in the focused field, and two strong areas become stronger with an increase in coherence length δ .

The analytical expressions for the cross-spectral density matrix of aberrated, partially coherent, electromagnetic, square, flat-topped pulsed beams focused by a thin lens have been derived. These analytical expressions

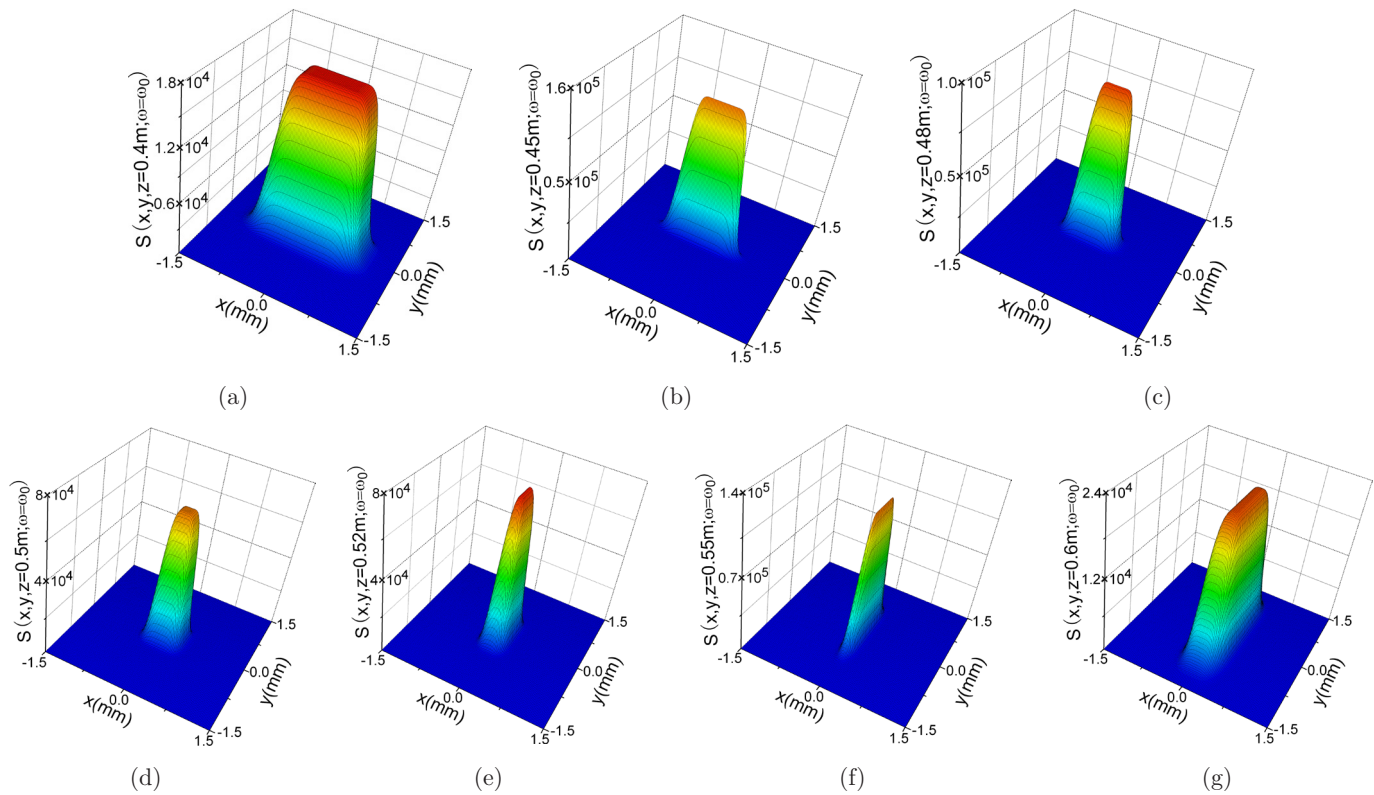


Fig. 4. (Color online) 3D irradiance spectral density distribution in the $x - y$ plane in the aberration case of $C_6 = 0.03 \text{ m}^{-1}$. (a) $z = 0.4 \text{ mm}$, (b) $z = 0.45 \text{ mm}$, (c) $z = 0.48 \text{ mm}$, (d) $z = 0.5 \text{ mm}$, (e) $z = 0.52 \text{ mm}$, (f) $z = 0.55 \text{ mm}$, and (g) $z = 0.6 \text{ mm}$. The other parameters are the same as in Fig. 2.

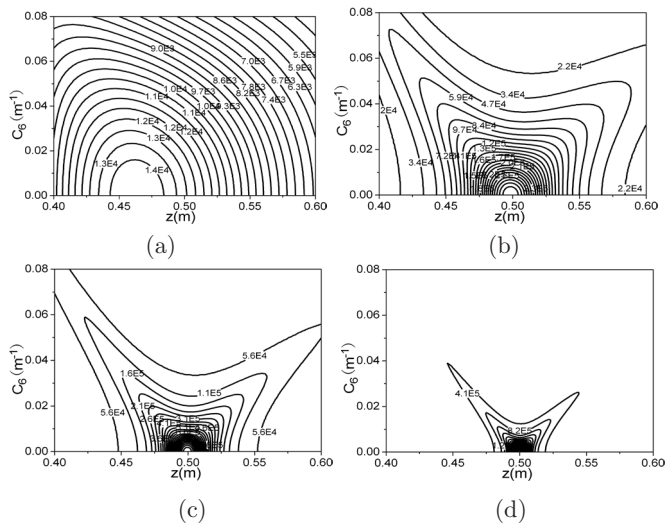


Fig. 5. Influence of the coherence length δ on astigmatism. (a) $\delta = 0.1 \text{ mm}$, (b) $\delta = 0.5 \text{ mm}$, (c) $\delta = 1 \text{ mm}$, (d) $\delta = 3 \text{ mm}$. The other parameters are $\sigma = 5 \text{ mm}$, $T_0 = 70 \text{ fs}$, $T_{cx} = T_{cy} = 4 \text{ fs}$, $A_x = A_y = 1$, $\omega_0 = 3.106 \text{ rad/fs}$, $\omega_1 = \omega_2 = \omega_0$, $f = 500 \text{ mm}$, and $N = 10$.

provide a convenient and effective way to study the propagation properties of this type of pulse beams. Not only the spectral density but also other focused properties such as spectra, coherence, and polarization are characterized in this study. However, with a number of

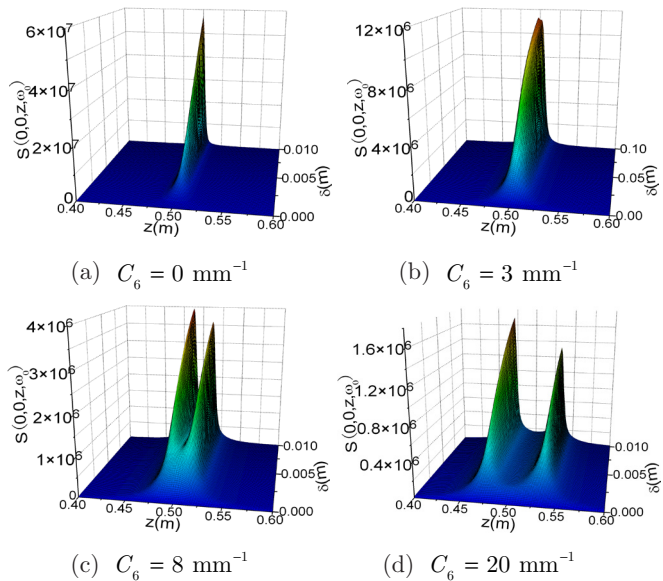


Fig. 6. (Color online) 3D irradiance spectral density distribution for different values of C_6 . (a) $C_6 = 0 \text{ mm}^{-1}$, (b) $C_6 = 3 \text{ mm}^{-1}$, (c) $C_6 = 8 \text{ mm}^{-1}$, and (d) $C_6 = 20 \text{ mm}^{-1}$. The other parameters are $\sigma = 5 \text{ mm}$, $T_0 = 70 \text{ fs}$, $T_{cx} = T_{cy} = 4 \text{ fs}$, $A_x = A_y = 1$, $\omega_0 = 3.106 \text{ rad/fs}$, $\omega_1 = \omega_2 = \omega_0$, $f = 500 \text{ mm}$, $N = 10$, and $\delta = 1 \text{ mm}$.

calculations, we mainly illustrate how the parameters of aberrated beams have effect on the spectral density in the focused field. Other propagation properties will be

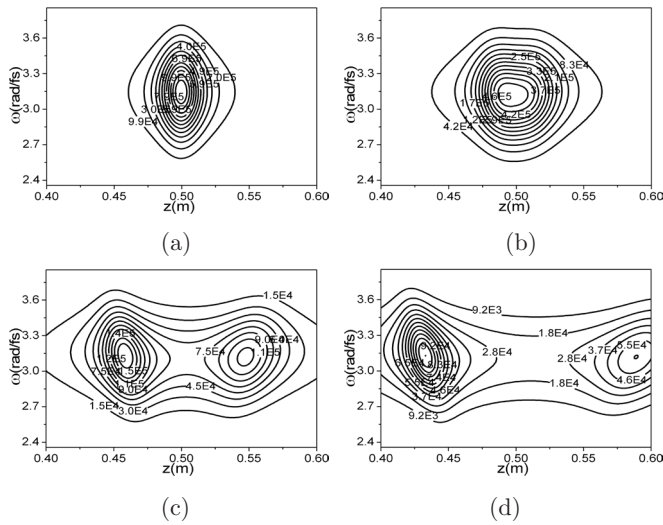


Fig. 7. Influence of the astigmatism coefficient C_6 on the frequency. (a) $C_6 = 0 \text{ mm}^{-1}$, (b) $C_6 = 0.01 \text{ mm}^{-1}$, (c) $C_6 = 0.03 \text{ mm}^{-1}$, (d) $C_6 = 0.05 \text{ mm}^{-1}$. The other parameters are $\sigma = 5 \text{ mm}$, $T_0 = 70 \text{ fs}$, $T_{cx} = T_{cy} = 4 \text{ fs}$, $A_x = A_y = 1$, $\omega_0 = 3.106 \text{ rad/fs}$, $\omega_1 = \omega_2 = \omega_0$, $f = 500 \text{ mm}$, $N = 10$, and $\delta = 1 \text{ mm}$.

considered in future work. Light source parameters, especially correlation length and astigmatism, are shown to determine the distribution of the aberrated, partially coherent, electromagnetic, square, flat-topped pulsed beams in the focused field. The dual-focus phenomenon caused by the astigmatism of the beams has been explained more clearly in this study than in the other references used in this paper. In certain circumstances, astigmatism is not necessarily undesirable, and a certain amount of astigmatism can guarantee a similar spatial envelope of the beams in the geometric focal plane as the source of square, flat-topped pulsed beams. This feature may be useful in determining the fidelity of high-power laser beam transmission areas.

The research was supported by the National Natural Science Foundation of China (Grant No. 60707019).

References

1. M. S. Bowers, *Opt. Lett.* **19**, 1319 (1992).
2. F. Gori, *Opt. Commun.* **107**, 335 (1994).
3. V. Baginni, R. Borghi, F. Gori, A. M. Pacileo, M. Santarsiero, D. Ambrosini, and G. Schirripa, *J. Opt. Soc. Am. A* **13**, 1385 (1996).
4. Y. Li, *Opt. Lett.* **27**, 1007 (2002).
5. Y. Li, *Opt. Commun.* **206**, 225 (2002).
6. Y. Cai and Q. Lin, *J. Opt. A: Pure Appl. Opt.* **6**, 390 (2004).
7. Y. Cai and S. He, *J. Opt. Soc. Am. A* **23**, 2623 (2006).
8. Y. Cai, X. Lu, H. T. Eyyuboglu, and Y. Baykal, *Opt. Commun.* **281**, 3221 (2008).
9. F. Wang and Y. Cai, *Opt. Lett.* **33**, 1795 (2008).
10. X. Ji, and B. Lv, *IEEE J Quantum Electron.* **39**, 172 (2003).

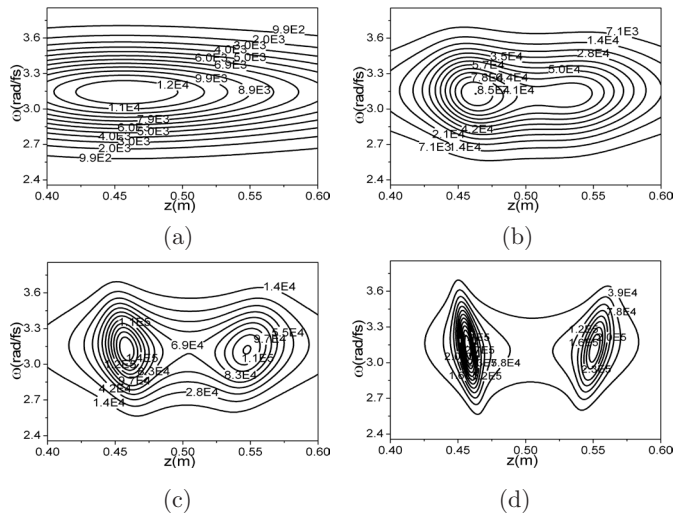


Fig. 8. Influence of the coherence length δ on the frequency for the astigmatism coefficient $C_6 = 0.03 \text{ mm}^{-1}$. (a) $\delta = 0.1 \text{ mm}$, (b) $\delta = 0.5 \text{ mm}$, (c) $\delta = 1 \text{ mm}$, (d) $\delta = 3 \text{ mm}$. The other parameters are $\sigma = 5 \text{ mm}$, $T_0 = 70 \text{ fs}$, $T_{cx} = T_{cy} = 4 \text{ fs}$, $A_x = A_y = 1$, $\omega_0 = 3.106 \text{ rad/fs}$, $\omega_1 = \omega_2 = \omega_0$, $f = 500 \text{ mm}$, and $N = 10$.

11. R. Borghi, M. Santarsiero, and S. Vicalvi, *Opt. Commun.* **154**, 243 (1998).
12. G. Wu, Q. Lou, J. Zhou, J. Dong, Y. Wei, and Z. Su, *Opt. Laser Technol.* **40**, 494 (2008).
13. B. Ghafary, H. Siampoor, and M. Alavinejad, *Opt. Laser Technol.* **42**, 755 (2010).
14. C. Zhao, Y. Cai, X. Lu, and H. T. Eyyuboglu, *Opt. Express* **17**, 1753 (2009).
15. H. T. Eyyuboglu, A. Arpali, and Y. Baykal, *Opt. Express* **14**, 4196 (2006).
16. P. Zhou, Y. Ma, X. Wang, H. Ma, X. Xu, and Z. Liu, *Appl. Opt.* **48**, 5251 (2009).
17. Y. Gao, B. Zhu, D. Liu, and Z. Lin, *Opt. Express* **17**, 12753 (2009).
18. L. Mandel and E. Wolf, Cambridge, NY, 1995.
19. Z. Y. Chen and J. X. Pu, *J. Opt. A: Pure Appl. Opt.* **9**, 1123 (2007).
20. W. Atsushi, O. Takumi, M. Yoko, and T. Mitsuo, *J. Opt. Soc. Am. A* **22**, 2746 (2005).
21. F. D. Kashani, M. Alavinejad, and B. Ghafary, *Optics Communications* **282**, 4029 (2009).
22. R. K. Singh, P. Senthikumar, and K. Singh, *J. Opt. A: Pure Appl. Opt.* **9**, 543 (2007).
23. C. Ding and B. Lv, *Optics and Lasers in Engineering* **47**, 673 (2009).
24. H. Yan and B. Lv, *J. Opt. Soc. Am. B.* **27**, 375 (2010).
25. H. Yan and B. Lv, *J. Opt. A: Pure Appl. Opt.* **11**, 065706 (2009).
26. H. Yan and B. Lv, *Opt. Commun.* **282**, 717 (2009).
27. L. Wang, M. Li, X. Wang, and Z. Zhang, *Optics laser Technology* **41**, 586 (2009).
28. A. Y. Bekshaev, M. S. Soskin, and M. V. Vasnetsov, *Opt. Commun.* **241**, 237 (2004).
29. L. Z. Pan, M. L. Sun, C. L. Ding, Z. G. Zhao, and B. D. Lv, *Optics express* **17**, 7310 (2009)